J Neurophysiol 95: 2314–2325, 2006.
First published November 30, 2005; doi:10.1152/jn.01007.2005.

Differential Receptor Activation by Cockroach Adipokinetic Hormones Produces Differential Effects on Ion Currents, Neuronal Activity, and Locomotion

Dieter Wicher,[1] Hans-Jürgen Agricola,[2] Sandra Söhler,[3] Matthias Gundel,[2] Stefan H. Heinemann,[4] Leo Wollweber,[5] Monika Stengl,[3] and Christian Derst[1,6]

[1]*Department of Neurohormones, Saxon Academy of Sciences, Jena;* [2] *Institute of Zoology, Friedrich Schiller University, Jena;* [3] *Institute of Animal Physiology, Philipps University Marburg, Marburg;* [4] *Institute of Molecular Cell Biology, Medical Faculty of the Friedrich Schiller University, Jena;* [5] *Institute of Molecular Biotechnology, Jena; and* [6] *Center for Anatomy, Charité Berlin, Berlin, Germany*

Submitted 29 September 2005; accepted in final form 28 November 2005

Wicher, Dieter, Hans-Jürgen Agricola, Sandra Söhler, Matthias Gundel, Stefan H. Heinemann, Leo Wollweber, Monika Stengl, and Christian Derst. Differential receptor activation by cockroach adipokinetic hormones produces differential effects on ion currents, neuronal activity, and locomotion. *J Neurophysiol* 95: 2314–2325, 2006. First published November 30, 2005; doi:10.1152/jn.01007.2005. Adipokinetic hormone (AKH) peptides in insects serve the endocrine control of energy supply. They also produce, however, neuronal, vegetative, and motor effects, suggesting that AKHs orchestrate adaptive behavior by multiple actions. We have cloned, for *Periplaneta americana*, the AKH receptor to determine its localization and, based on current measurements in neurons and heterologous expression systems, the mechanisms of AKH actions. Apart from fat body, various neurons express the AKH receptor, among them abdominal dorsal unpaired median (DUM) neurons, which release the biogenic amine octopamine. They are part of the arousal system and are involved in the control of circulation and respiration. Both the two *Periplaneta* AKHs activate the G_s pathway, and AKH I also potently activates G_q. AKH I and—with much less efficacy—AKH II accelerate spiking of DUM neurons through an increase of the pacemaking Ca^{2+} current. Because the AKHs are released from the corpora cardiaca into the hemolymph, they must penetrate the blood–brain barrier for acting on neurons. That this happens was shown electrophysiologically by applying AKH I to an intact ganglion. Systemically injected AKH I stimulates locomotion potently in striking contrast to AKH II. This behavioral difference can be traced back conclusively to the different effectiveness of the AKHs on the level of G proteins. Our findings also show that AKHs act through the same basic mechanisms on neuronal and nonneuronal cells, and they support an integration of metabolic and neuronal effects in homoeostatic mechanisms.

INTRODUCTION

Peptide hormones play an important role in energy homeostasis and, thereby, orchestrate different processes within one main physiological context. Similar to glucagon in mammals—although in a less complex fashion—the insect adipokinetic hormones (AKHs) regulate energy homeostasis. They mobilize energy reserves from storages, particularly from the fat body (Gäde et al. 1997; Van der Horst et al. 2001). In *Drosophila*, AKH, however, also acts as a command to enhance locomotor activity on starvation that may help to find food (Lee and Park 2004). This is but one example for a central nervous role of AKHs (cf. Kodrik et al. 2000; Milde et al. 1995). AKHs are produced in endocrine cells of the corpora cardiaca (CC) and are released into the hemolymph (Schooneveld et al. 1983), and it seems conceivable that circulating AKH can affect neurons.

In insects there is an octopaminergic arousal system of ~100 distributed neurons in the brain and ventral nerve cord that up-regulates general activity levels comparable with the noradrenergic system in mammals (Roeder 2005). Octopamine is a stress signal that primes the animal for "fight or flight" and elicits enhanced locomotor output activity (Saraswati et al. 2004; Stevenson et al. 2005). In addition, octopamine from dorsal or ventral unpaired median (DUM or VUM) neurons in segmental ganglia is specifically targeted, as a modulator, to various peripheral organs, particularly to the heart and to muscles involved in ventilation, locomotion, or flight (Bräunig and Pflüger 2001).

The abdominal DUM neurons of the cockroach *Periplaneta americana* are octopaminergic neurosecretory cells acting on muscles of the ventilatory system and on the heart, i.e., they play important general roles in regulatory physiology (Nässel 1996; Roeder 2005). For cockroach abdominal DUM neurons, a large fraction of the ionic currents have been characterized in detail (Grolleau and Lapied 2000; Wicher et al. 2001) and several of these ionic currents are affected by AKH I (also named neurohormone D; Baumann and Penzlin 1984), one of the two adipokinetic hormones produced in *Periplaneta* (Wicher et al. 2001).

To address the complex problem of hormonal regulation of neuronal activity in the context of homeostasis, we have applied a facet of experimental approaches, starting from the molecular cloning of the cockroach AKH receptor, its functional characterization with respect to the type of G protein coupling elicited by both AKHs, the differential regulation of DUM neurons by AKHs and to the behavioral effects of AKHs on *Periplaneta* locomotor activity. We conclude that AKHs affect the physical activity of the animals by differentially activating a pacemaking current in DUM neurons.

Address for reprint requests and other correspondence: D. Wicher, Max Planck Institute for Chemical Ecology, Hans-Knöll-Str. 8, 07745 Jena, Germany (E-mail: dwicher@ice.mpg.de).

The costs of publication of this article were defrayed in part by the payment of page charges. The article must therefore be hereby marked "*advertisement*" in accordance with 18 U.S.C. Section 1734 solely to indicate this fact.

METHODS

Cloning of the Periplaneta *adipokinetic hormone receptor*

Two sets of degenerated primers were designed for a nested PCR approach, according to the AKHR sequences of *Bombyx mori*, *Anopheles gambiae,* and *Drosophila melanogaster* (IUB 1 letter code): FOR-1, 5′-TGATGCCRMTGGAGAT-3′; FOR-2, 5′-TTYGGVCTKTAYCT-GTCCAGCT-3′; BACK-1, 5′-GASTSCTTGTCVAKCCARTACCA-3′; BACK-2, 5′-GTAGTABGGMGWCCAGCA-3′.

Both PCR reactions were performed with initial 6-min 94°C enzyme activation followed by 40 cycles with 30 s for 94°C, 30 s for 50°C, and 1 min for 72°C using AmpliTaq Gold Polymerase (Applied Biosystems, Darmstadt, Germany). The amplified 480-bp product was cloned into pBluescript SK+ and sequenced. To amplify 5′ and 3′ cDNA ends a nested RACE approach was used as described previously (Derst et al. 2003). The following four primers were designed: RACE-F1, 5′-CTCAACAGGGCCAGGAATAGGACTCTCAA-3′; RACE-F2, 5′-ATGGCCATCATCATATTCGTCGTATTCTTC-3′; RACE-B1, 5′-AGCATCAGTTTGCCTCGACGCGCCAC-3′; RACE-B2, 5′-TG-GACATGGGTCGCAGGATG-3′.

Both RACE reactions were performed using the AdvantageTaq 2 Polymerase Mix (Clontech, Palo Alto, CA) for 40 cycles with 30 s for 94°C, 30 s for 66°C, and 4 min for 68°C. RACE products were directly sequenced. For construction of a full-length AKHR expression vector two primers with incorporated restriction sites for *Eco*RI and *Xho*I were designed: FL-F1, 5′-TAACGAATTCATGGCGT-TATCCAGTTGCAG-3′; FL-B1, 5′-CGTGCTCGAGTCATCTGCA-GATGACAGAAG-3′.

PCR reaction was performed for 40 cycles with 30 s for 94°C, 30 s at 60°C, and 2 min at 68°C using AdvantageTaq 2. The PCR product was purified, digested with *Eco*RI and *Xho*I, and cloned into the expression vector pcDNA3.1(+).

RT-PCR analysis of pAKHR expression

A nested RT-PCR approach was developed for testing tissue and ganglion specific expression and single cell analysis of isolated DUM neurons. The following PCR primers were designed: Sc-F1, 5′-CGCTACGGCAACAACTACAT-3′; Sc-F2, 5′-CTTGCTGGT-GACGTTCTTGA-3′; Sc-B1, 5′-CAAGGATCCAGGCCACAGT-3′; Sc-B2, 5′-GAGCATCAGTTTGCCTCGAC-3′.

RNA was isolated from different tissues and from thoracic and abdominal ganglia using the RNeasy Mini Kit (Qiagen, Hilden, Germany). For single-cell RT-PCR analysis, the cytosol of single DUM neurons was harvested with patch pipettes and directly transferred to the RT reaction mixture. RT reaction was performed with either Superscript II reverse transcriptase (Invitrogen, Karlsruhe, Germany) and tissue/ganglion RNA or with Sensiscript reverse transcriptase (Qiagen) and isolated cytosol of single DUM neurons, respectively. The nested PCR reactions were performed with AmpliTaq Gold Polymerase (Applied Biosystems) with an initial 6 min for 94°C enzyme activation followed by 40 cycles 30 s for 94°C, 30 s for 55°C, and 1 min for 72°C. PCR products of the second PCR reaction were visualized on a 2% agarose gel and directly sequenced to confirm the correct specificity.

As a positive control, we amplified part of a ubiquitously expressed actin gene from *P. americana*. To exclude false-positive results caused by genomic DNA contamination, PCR primers were intron-spanning. The position of the intron, deduced from *Drosophila* and *Anopheles* genomic sequences, was verified by a PCR reaction with 8-min elongation and *Periplaneta* genomic DNA as template. The resulting ~3-kB fragment was cloned into pGEM-T and intron position confirmed by sequencing (sequence deposited under GenBank accession no. AY566245).

Staining of DUM neurons

Neurons were identified using the differential staining according to (Sakai and Yamaguchi 1983). The nerve trunks of the sixth abdominal ganglion were draped over a barrier of vaseline and placed in two different chambers containing a 1 M $NiCl_2$ or 1 M $CoCl_2$ solution, respectively. Preparations were kept in a refrigerator at 4°C for 24–48 h. They were washed and developed for 15 min in a solution of sodium cacodylate buffer (3 ml, 0.15 M, pH 7.4) containing 8% sucrose plus three to four drops of saturated alcoholic rubeanic acid solution. After washing, the tissue was fixed in Carnoy's solution for 20 min, dehydrated in ethanol, and cleared in methyl salicylate. The whole mount preparations were intensified with silver (Bacon and Altman 1977) and analyzed with a Wild M10 stereomicroscope (including camera lucida attachment) and a Zeiss Jenaval photomicroscope.

Antibody production and immunocytochemistry

PRODUCTION OF THE MONOCLONAL OCTOPAMINE ANTIBODY MAB-OA1. The production and test for specificity is described in Dacks et al. (2005).

PRODUCTION OF THE AKH I ANTIBODY. An anti-AKH I serum was raised in rabbits against the conjugate from synthetic PVNF-SPNWamide-glutaraldehyde-thyroglobuline.

PRODUCTION OF THE pAKHR ANTIBODY. Two anti-pAKHR sera were raised in rabbits against the synthetic peptide VTWYEQCVS-FNFFS (AB1) corresponding to part of the loop between the fourth and the fifth transmembrane domain of pAKHR and against the C-terminal motif GRRNSRET (AB2). The peptides were cross-linked to keyhole limpet hemocyanin (KLH) by means of glutaraldehyde. AB1 was produced by Sigma-Genosys (Cambridge, UK). The peptide and the conjugate for production of AB2 was provided by Biotrend (Köln, Germany), and the antiserum was produced in our laboratory.

WESTERN BLOT. Three freshly isolated cockroach ganglia or HEK293 cells transfected with pAKHR/pcDNA3.1 were homogenized in 50 μl lysis buffer (50 mM Tris, 150 mM NaCl, 5 mM EDTA, 1 mM EGTA, 1% Triton X-100, 1 tablet per 50 ml Complete Protease Inhibitor Cocktail; Roche Diagnostics, Mannheim, Germany). Ten microliters was loaded on a 10% SDS-PAGE for separation of proteins. After electrophoresis, the proteins were transferred at 2 mA/cm^2 to an Immobilon-P membrane (Millipore, Eschborn, Germany) using a *trans*-Blot SD Semi-Dry Electrophoretic Transfer Cell (BioRad, München, Germany). After the blotting procedure, the membrane was preincubated in 4% BSA in PBS containing 0.2% Tween-20 (PBS-T) over night. A 1:500 dilution of the pAKHR-specific antibody AB1 in PBS-T was used for detection of pAKHR (1 h, room temperature). After five wash steps with PBS-T, the membrane was incubated for 45 min with an anti-rabbit IG-horseradish peroxidase conjugate (Amersham, Freiburg, Germany) as a secondary antibody followed by another five wash steps with PBS-T. Finally, the ECL plus Western Blotting Detection System (Amersham) was used to detect pAKHR bands.

IMMUNOCYTOCHEMISTRY—OCTOPAMINE. For this information, see Supplementary Material[1] and Dacks et al. (2005). Brains, ventral nerve cords, and ganglia were fixed in 4% formaldehyde in 0.1 M Millonigs buffer (pH 7.3–7.4) overnight at room temperature. The preparations were washed in Tris-HCl buffer (pH 7.4, 146 mM NaCl, 50 mM Tris-OH) for 12 h at 4°C on a shaker. Forty-micrometer-thick sections of agar-embedded tissues were cut on a vibratome (Technical Products, St. Louis, MO). The washed free-floating vibratome sections were incubated in rabbit anti-pAKHR or anti-AKH-polyclonal

[1] The Supplementary Material for this article (four figures) is available online at http://jn.physiology.org/cgi/content/full/01002.2005/DC1.

antibody diluted each 1:1,000 in a solution of Tris-HCl buffer containing 2% normal goat serum, 0.25% Triton-X, 3% skim milk powder, and 0.25% bovine serum albumin (MPB). Subsequently, the tissue was washed in the MPB overnight and incubated in the Cy3 tagged secondary antibody (Jackson ImmunoResearch) for 3 h at a dilution of 1:800 in MPB. The vibratome sections were mounted and embedded in mowiol.

For the photographic documentation, we used the bright-field optics on a Zeiss Axiophot microscope, a Hammamatsu digital camera C4742-95, and the software OpenLab (Improvision, Coventry, UK).

Heterologous expression of AKH receptor in HEK293 cells

HEK293 cells were cultured at a density of $\sim 2 \times 10^4$ per 35-mm dish and transfected with 1 μg pAKHR/pcDNA3.1 and 0.8 μg pEGFP-C1 (Clontech) using SuperFect (Qiagen). In addition, we transfected cells with either 2.5 μg hHCN2/pcDNA3 (provided by M. Biel, Munich, Germany) or with 1 μg hKCNQ4/pcDNA3.1.

Electrophysiology

Ion currents in HEK293 cells and in DUM neurons (isolated according to Wicher et al. 1994) were measured at room temperature using whole cell patch clamp with appropriate compensation of series resistance and of capacitive and leakage currents. Pipettes having resistances of 2–4 MΩ (HEK293 cells) or 0.5–0.8 MΩ (DUM cells) were pulled from borosilicate capillaries. Current measurements and data acquisition were performed using an EPC9 patch-clamp amplifier controlled by PULSE software (HEKA Elektronik, Lambrecht, Germany).

HEK293 CELLS. For experiments with KCNQ channels, the pipette solution contained (in mM) 140 KCl, 4 NaCl, 2 Mg-ATP, 2.2 $CaCl_2$, 5 EGTA, and 10 HEPES (pH = 7.3), and the bath solution contained (in mM) 135 NaCl, 5 KCl, 1 $MgCl_2$, 1 $CaCl_2$, 10 glucose, and 10 HEPES (pH = 7.4). Experiments with hyperpolarization-activated cyclic nucleotide-gated (HCN) channels were performed with the above pipette solution and K^+-rich bath solution differing from the above solution by 110 mM NaCl and 30 mN KCl. For this combination, the K^+ equilibrium potential was –39 mV.

DUM NEURONS. Spiking of neurons was recorded under current-clamp conditions without current injection. The bath solution contained (in mM) 190 NaCl, 5 KCl, 5 $CaCl_2$, 2 $MgCl_2$, and 10 HEPES (pH = 7.4), and patch pipettes (resistance >1.5 MΩ) were filled with solution composed of (in mM) 190 K-gluconate, 5 NaCl, 2 Mg-ATP, 1 $CaCl_2$, 3 EGTA, and 10 HEPES (pH = 7.25). Between recordings (duration 1 s), the cells were held under voltage clamp at a holding potential of −70 mV.

Na^+ currents were separated as described (Wicher 2001a) with pipette solution composed of (in mM) 5 NaCl, 100 choline methylsulfate, 30 TEA-Br, 3 CsCl, 60 CsOH, 2 Mg-ATP, 1 $CaCl_2$, 5 EGTA, and 10 HEPES and bath solution containing (in mM) 60 Na isethionate, 90 choline methylsulfate, 40 TEA-Br, 7 $MgCl_2$, 1 $CdCl_2$, and 10 HEPES. For Ca^{2+} current measurements (Wicher and Penzlin 1997), the pipette solution contained (in mM) 100 choline methylsulfate, 30 TEA-Br, 8 CsCl, 60 CsOH, 2 Mg-ATP, 1 $CaCl_2$, 5 EGTA, and 10 HEPES, and the bath solution contained (in mM) 5 $CaCl_2$, 190 choline methylsulfate, 10 HEPES, and 5 μM TTX.

EXTRACELLULAR RECORDINGS. The output of neurons from the sixth abdominal ganglion projecting into segmental nerves was recorded using pipettes with 0.3-MΩ resistance when filled with bath solution. To get access to segmental nerves, animals were fixed, and a tiny ventrally located window was set. Recordings were performed from the mean and the posterior branch of segmental nerves that contain the axons of the three large DUM neurons (see Supplementary Fig. 2).

Locomotor activity

Locomotor activity of 20 male cockroaches (*Periplaneta americana*) was monitored in running wheels in constant darkness at 27°C (Stengl and Homberg 1994). After fast anesthesia by ice water, we dorsally injected 1 μl of 2 μM AKH I, 2 μM AKH II, or saline (control injection) between meso- and metathorax. Test injections with 1 μl saline containing methylene blue into the same injection site in the thorax revealed that it took between 30 min and 1 h to observe staining in the ventral nerve cord ($n = 5$ animals). The same number of control injections, AKH I, and AKH II injections were always performed at the same Zeitgebertime into different animals to allow statistical analysis. After injection, the animals were immediately returned to the running wheel. Data were evaluated from records with at least episodic circadian activity before and after the injection ($n = 37$). Animals were injected at Zeitgebertime X (ZT X), either during their resting phase (at ZT 0–12, with ZT 0 lights on and ZT 12 lights off), or during their activity phase (ZT 12–24). Time bins of 6 h were averaged before and after injection. Means of the running wheel activity within ZT X and ZT X + 6 h were averaged over 4 days before the day of injection (basal activity). Mean locomotor activities within ZT X and ZT X + 6 h were normalized to basal activity and statistically analyzed using one-way ANOVA. All data collected before the activity phase were pooled peptide—specifically separately from the data of the inactivity phase.

Chemicals

AKH I and AKH II were obtained from Peninsula (Heidelberg, Germany), pertussis toxin (PTX) and TTX were from Sigma, and U73122 was from RBI (Natick, MA).

Data analysis

Results are given as means ± SE (n = number of cells). The evaluation of statistical significance of differences was performed with two-way ANOVA.

Current-voltage (I-V) relationships for Na^+ and Ca^{2+} peak currents were fitted taking into account current rectification according to a Goldman-Hodgkin-Katz (GHK)-model of the form

$$I(V) = GV\{[1 - \exp(-(V - V_{rev})/Z)]/[1 - \exp(-V/Z)]\} \times \{1/[1 + \exp(-(V - V_{0.5})/S)]\}$$

where G is the total conductance, V_{rev} is the reversal potential, $V_{0.5}$ is the potential for half-maximal activation of total conductance, and S is the slope factor of activation. The abbreviation Z stands for RT/zF, where z is the valence of the ion and RT/F = 25 mV at room temperature.

Activation curves were fitted with a Boltzmann equation according to

$$G/G_{max} = 1/\{1 + \exp[-(V - V_{0.5})/S]\}$$

where G_{max} is the maximal conductance, $V_{0.5}$ is the voltage of half-maximal activation, and S the slope factor.

The time-course of the peptide-induced increase in spike frequency f of DUM neurons was described by

$$(f - f_{Con})/(f_{max} - f_{Con}) = (1 - \exp[-(t - del)/\tau])$$

where f is the frequency at time t, f_{Con} is the frequency before peptide application, f_{max} is the maximum frequency attained in the presence of peptide, del is the delay, and τ is the time constant.

RESULTS

Sequence analysis of the pAKHR

AKH receptors (AKHRs), which activate heterotrimeric G_q and G_s proteins to mobilize energy (Gäde and Auerswald 2003;

Van der Horst et al. 2001), are presently known only in *Drosophila* and the silkworm *Bombyx mori* (Staubli et al. 2002). Using a combined degenerated PCR-RACE protocol, we isolated the 1,760-bp full-length cDNA encoding the 456 amino acid *P. americana* adipokinetic hormone receptor (pAKHR; GenBank accession no. AY286427). The pAKHR showed all typical structural features of G protein–coupled receptors: extracellular N terminus, seven transmembrane regions, and a large intracellular C terminus. On the amino acid level, pAKHR showed highest homology to the orthologous sequences from *Drosophila* (42.6% identity, 51.5% similarity), *Bombyx* (44.5% identity, 52.9% similarity), and *Anopheles* (49.5% identity, 59.1% similarity). For details, see Supplementary Fig. S1.

G protein coupling of the AKH receptor

Two recently developed algorithms aimed of predicting the G protein specificity of receptor coupling were applied to analyze the sequence of pAKHR. GRIFFIN (G protein and receptor interaction feature finding system; Yabuki et al. 2005) predicted a coupling to G_s. Because this algorithm stops on identifying G_s-binding type, it does not provide information on possible other G protein coupling. The algorithm PRED-COUPLE (Sgourakis et al. 2005), which is also able to model promiscuous coupling, predicted a further coupling specificity of pAKHR for G_q.

To analyze coupling of pAKHR to G_s and G_q proteins experimentally, pAKHR was coexpressed with ion channels known to be modulated through G_s or G_q proteins in HEK293 cells. The human hyperpolarization activated cyclic nucleotide-gated channel (hHCN2) served as sensor for G_s coupling, whereas the voltage-gated channel hKCNQ4 was used to probe for G_q stimulation. Without the expression of pAKH receptor application of 10 nM AKH I, neither affected hHCN2 currents ($n = 4$) or hKCNQ4 currents ($n = 4$), ruling out an endogenous AKH recognizing receptor in HEK293 cells.

G_S COUPLING. A rise in cAMP level shifts the activation curve of HCN channels to more positive potentials and leads to more rapid activation kinetics (Accili et al. 2002). If the pAKH receptors couple to G_s, one expects that AKH binding enhances cAMP production and thus modulates hHCN2 currents. Indeed, both AKH I and II lead to faster activation kinetics and did so to the same extent (Fig. 1*A*). The activation time constant at –120 mV was reduced from 279 ± 14 to 221 ± 24 (AKH I, $n = 5$) and 219 ± 22 ms (AKH II, $n = 5$). The peptides also caused a depolarizing shift of the activation curve (Fig. 1*B*). AKH I and II shifted $V_{0.5}$ by 11.0 ± 2.6 ($n = 5$) and 11.2 ± 2.6 mV ($n = 5$), respectively (Fig. 1*B*). For comparison, intracellular perfusion with 1 mM cAMP of hHCN2 channels expressing HEK293 cells caused a shift of +16 mV (Ludwig et al. 1999). Taken together, both AKHs appeared to have the same effect on pAKHR-G_s coupling.

G_Q COUPLING. KCNQ channels are voltage-gated outwardly rectifying K^+ channels that are inhibited on activation of G_q proteins. This has been shown for human KCNQ1-4 channels heterologously coexpressed in CHO cells with M_1 muscarinic acetylcholine receptors (Selyanko et al. 2000). We coexpressed hKCNQ4 channels with pAKHR to study G_q activation. AKH I much more effectively depressed the KCNQ currents than

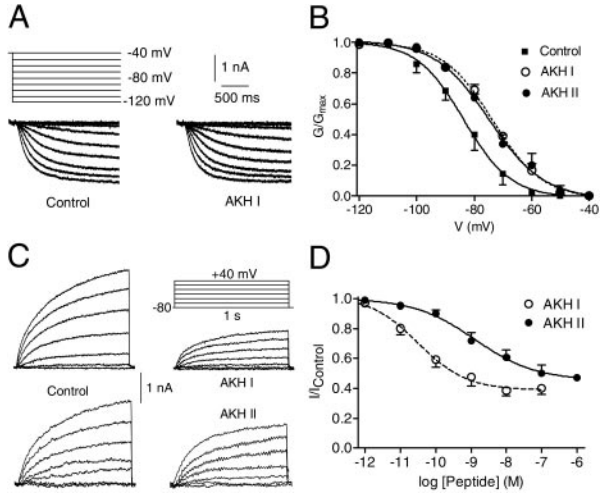

FIG. 1. Test for G protein coupling of *Periplaneta* adipokinetic hormone receptor (pAKHR) in HEK293 cells. Channels were coexpressed with pAKHR in HEK293 cells. *A*: family of hHCN2 currents obtained by the indicated pulse protocol before and after application of 10 nM adipokinetic hormone (AKH) I. *B*: normalized tail currents as a function of test voltage (G-V). Superimposed Boltzmann functions (*Eq. 2*) are characterized by $V_{0.5}$ of –84, –73, and –74 mV and by slope of 8.1, 8.6, and 9.3 mV for control, 10 nM AKH I, and 10 nM AKH II, respectively. $n = 5$. *C*: families of hKCNQ4 currents activated by the indicated pulse protocol before and after application of AKH I or AKH II. *D*: concentration dependence of the effects of AKH I and AKH II on the current amplitude at +40 mV. Data were obtained from 5 to 7 cells; in each cell, ≤3 concentrations were tested. Fit curves correspond to IC_{50} of 31 pM and 1.3 nM and n_H of 0.63 and 0.50 for AKH I and AKH II, respectively. AKH I (10 nM) failed to reduce currents in cells not transfected with pAKHR cDNA (not shown, $n = 5$).

AKH II (Fig. 1, *C* and *D*). The IC_{50} was 31 pM for AKH I and 1.3 nM for AKH II (Fig. 1*D*). While the effect of AKH I saturated at ~10 nM (reduction by 62%), there was no saturation of the AKH II-effect ≤1 μM (reduction by 54%). Both dose–response relationships were significantly different (ANOVA, $P = 0.016$). The reduction of KCNQ currents by the AKHs was independent of voltage because the steady-state activation curves were not changed (data not shown). The kinetics of channel activation were not affected (Fig. 1*C*).

Activated G_q proteins, but also the βγ subunit of G_i proteins, stimulate phospholipase C (PLC) (Daaka et al. 1997). A switch from G_s to G_i coupling could, for example, occur at higher ligand concentration (Krsmanovic et al. 2003). To confirm that the AKH-induced reduction of KCNQ currents is a consequence of enhanced PLC activity, AKH I was applied in the presence of the PLC inhibitor U73122 (3 μM). Under these conditions, AKH I in fact failed to inhibit hKCNQ4 currents (98 ± 4% of control, $n = 4$). To test whether, in addition, G_i protein coupling of AKH receptor may be involved in the down-regulation of KCNQ current, HEK293 cells were pretreated with PTX (100 ng/ml) for 16 h. Application of 10 nM AKH I caused a mean reduction of KCNQ current to 48 ± 4% of control ($n = 6$), which did not significantly differ from the effect of AKH I in the absence of PTX (reduction to 38 ± 4% of control, $n = 6$; *t*-test, $P = 0.12$). Similarly, the AKH II effects on KCNQ currents were not affected by PTX (data not shown). There is thus no indication for an involvement of G_i protein activation by AKHs.

Taken together, the results have shown that, in the heterologous expression system, AKH binding to pAKHR activates G_s and G_q proteins. While both AKHs produced G_s activation

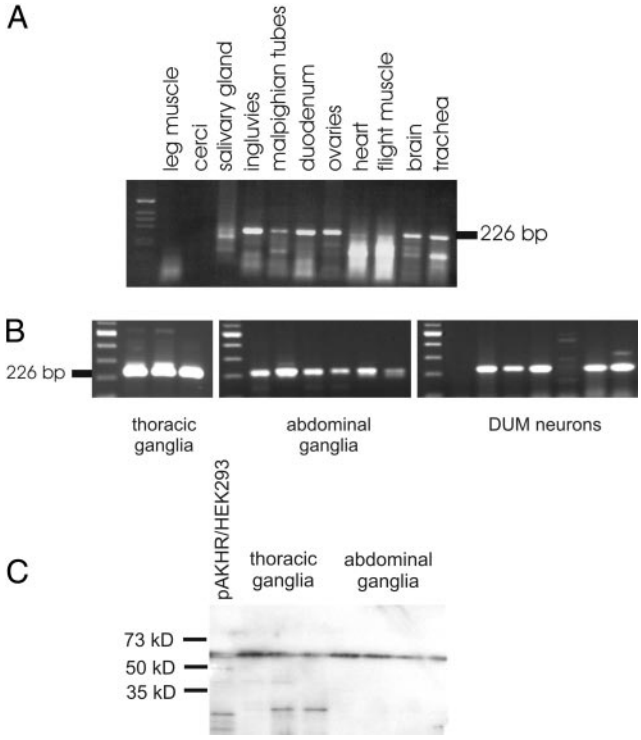

FIG. 2. Distribution of AKH receptors. *A*: RT-PCR analysis of the expression of pAKHR cDNA (226 bp) in different organs. Marker: 100-bp ladder. *B*: RT-PCR analysis in ventral nerve cord. A 226-bp PCR product was found in all abdominal and thoracic ganglia (*left*). Single cell RT-PCR identified pAKHR in 5 of 7 DUM neurons (*right*). *C*: Western blot analysis of pAKHR expression in isolated ganglia. A dominant ~58-kDa band was detected by AB1 in thoracic and abdominal ganglia as well as in pAKHR transfected HEK293 cells. Molecular weights of the protein marker are indicated.

with the same efficiency, AKH II had weaker capability than AKH I to induce pAKHR-G_q coupling.

Distribution of pAKHR

A nested PCR approach was used to test the expression of pAKHR. Expression was strong in brain, tracheae, ovaries, and digestive system. Weak expression was observed in salivary glands, malpighian tubules, heart, and flight muscles, and there was no expression in leg muscles (Fig. 2*A*). Besides in the brain, the pAKHR message was also pronounced in thoracic and abdominal ganglia (Fig. 2*B*). Because we were particularly interested in the actions of AKHs on DUM neurons, we performed single cell PCR on DUM cells isolated from the sixth abdominal ganglion to see if they express pAKHR—as has to be expected from the previously established modulatory effects of AKH I in these neurons (Wicher et al. 2001). In five of seven actin-positive cells, pAKHR was found (Fig. 2*B*).

On the protein level, a dominant ~58-kDa band was found in all thoracic and abdominal ganglia by Western blot analysis using a primary antibody against pAKHR (Fig. 2*C*). The same protein band was also detected in HEK293 cells overexpressing pAKHR.

Within the sixth abdominal ganglion, there are four octopaminergic DUM neurons (Eckert et al. 1992), their somata forming a cluster near the posterior end of the ganglion (Supplementary Fig. 2, *A* and *B*). According to soma size and projections into the segmental nerves three types of DUM neurons were found. Two large type 1 neurons (soma diameter 51 ± 6 μm, $n = 12$) project into all three segmental nerve branches (Supplementary Fig. 2C), one type 2 neuron (44 ± 3 μm, $n = 9$) sends processes into the middle and the posterior nerve branches (Supplementary Fig. 2*D*), and a small type 3 neuron (28 ± 4 μm, $n = 11$) projects into the anterior nerve branch A only (Supplementary Fig. 2*E*). The differences in size are reflected by different cell capacitances: 372 ± 58 ($n = 43$) for type 1 and type 2 cells and 212 ± 18 ($n = 13$) for type 3 cells. For electrophysiology, only type 1 and 2 cells were used.

The antibodies against pAKHR stained most neuronal somata and glial cells but not neuropile areas in all parts of the CNS. Both antibodies that were designed against different peptide motifs within the receptor protein recognized the same structures. As shown for the sixth abdominal ganglion, the intensity of immunostaining within the cytoplasm of cell bodies was considerably variable (Fig. 3, *A* and *B*). In control immunostainings with preimmune serum, we never observed immunoreactive granular structures in cytoplasm (Fig. 3, *C* and *D*). The nuclei did not show any pAKHR-immunostaining (Fig. 3*A*). Three DUM neurons displaying intense staining are shown in Fig. 3*A* (*inset*). Superposition of octopamine (Fig. 3*E*) and pAKHR-immunostaining (Fig. 3*F*) unequivocally showed that pAKHR is expressed in these neurons (Fig. 3*G*). As expected, there was also profound anti-pAKHR immunostaining at fat body cells (data not shown).

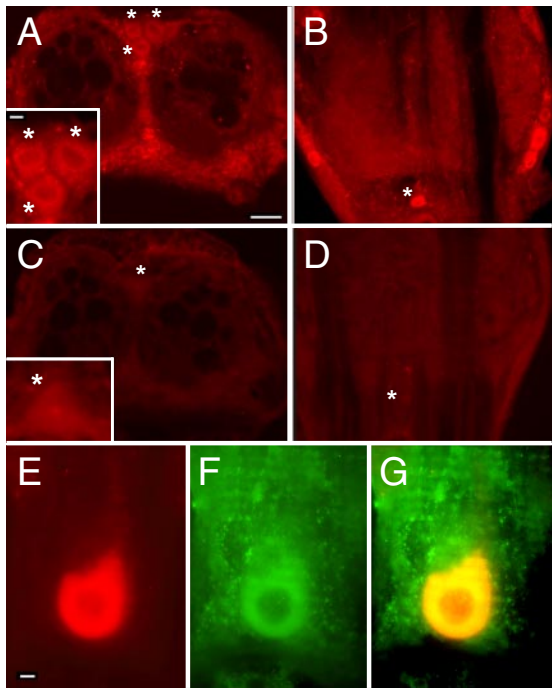

FIG. 3. AKH receptor expression in DUM neurons. *A* and *B*: anti-pAKHR immunofluorescence (AB2) in the 6th abdominal ganglion. *A*: frontal section. *B*: horizontal section. Immunofluorescence (Cy3) appears as granular structure within the cytoplasm of virtually all somata, yet with largely different intensity. *Position of DUM neurons. Calibration bar, 50 μm (*inset*: 10 μm). *C* and *D*: control staining of similar sections as in *A* and *B* using the preimmune serum of AB2. There is no specific immunofluorescence in the cytoplasm of cell bodies (*C*, *inset*). *DUM neurons. E–G: anti-octopamine immunofluorescence (*E*), anti-pAKHR immunofluorescence (AB1) (*F*), and superposition of both (*G*) in a DUM cell body. Calibration bar: 10 μm.

Distribution of AKH peptides

AKHs are produced by endocrine cells of the CC (Schooneveld et al. 1983). To determine whether AKHs might also be synthesized within the nervous system, we performed AKH I immunocytochemistry in embryonic and adult ventral nerve cords. In contrast to previous findings (Eckert et al. 1996), AKH I was not seen in brain and ventral nerve cord. It was exclusively found in the cytoplasm of the CC endocrine cells and their processes (Fig. 4*A*; $n = 20$ animals), which is in line with previous reports (Kim and Rulifson 2004; Lee and Park 2004). In *Drosophila,* there are intracerebral projections of the AKH producing CC cells (Lee and Park 2004). Such projections were, however, not seen in *Periplaneta*.

In conclusion, AKHs are not synthesized within the *Periplaneta* nervous system. At least for the ventral nerve cord, one has to assume that AKHs have to penetrate the blood–brain barrier to approach the AKH receptors expressed by so many neurons.

Access of AKH peptides to the CNS

To obtain evidence that AKH peptides are capable of crossing the ganglionic sheath, we applied AKH to the intact sixth abdominal ganglion while recording extracellularly from segmental nerves containing axons of DUM neurons. These previously have been shown to be stimulated by AKH I (Wicher et al. 2001). Their firing pattern could be easily identified by the large size of signals (Fig. 4*B*; cf. Ferber and Pflüger 1992). Under control conditions, the firing frequency of DUM neurons was 2.2 ± 0.9 Hz ($n = 7$). On application of AKH I (10 nM), the spike activity increased to 3.6 ± 1.2 Hz ($n = 7$). The effect started after a latency of about 2 min (Fig. 4, *B* and *C*), and thereafter, developed with a time-course similar to that in isolated DUM cells (Fig. 4*C*).

The enhanced neuronal activity on external peptide application shows the capability of AKH I to penetrate the sheath of the ganglion. An artifact caused by damage of sheath during preparation can be ruled out because application of the Na^+ channel blocker TTX did not affect spiking (data not shown). The extracellular recordings also indicated that the activity of non-DUM neurons became greatly increased because the frequency of small spikes was clearly enhanced 5 min after AKH I administration (Fig. 4*B*). That the effect of AKH peptides was not restricted to DUM neurons is in line with the results of pAKHR immunocytochemistry.

Effect of AKH peptides on spiking in DUM neurons

Because there are two AKHs in *Periplaneta,* AKH I and II, which are identical in the C-terminal region but different in the N-terminal region (Fig. 5*A*), we examined whether they affect electrical properties of DUM neurons differently. Under control conditions, isolated abdominal cockroach DUM neurons show spontaneous, tonic activity (Lapied et al. 1989; Wicher et al. 2006). Both AKHs modulated the discharge pattern by shortening the interspike interval (Fig. 5*B, left*) and by enhancing action potential (AP) hyperpolarization (Fig. 5*B, right*). However, the two AKHs accelerated spiking clearly differently: with a saturating effect in spike frequency increase by 26 ± 3% for AKH I and by 20 ± 3% for AKH II ($n = 10$), the EC_{50} for AKH I was 44 pM, whereas it was 1.0 nM for AKH II (Fig. 5*C*). Because the pacemaker depolarization essentially determines the spike frequency, we compared the effect of peptides on the slope of pacemaker depolarization with those on spike frequency. Under control conditions, the midpoint potential of the interspike interval was −42.1 ± 1.3 mV ($n = 10$). In the absence of peptides, the time derivative at −42 mV was 0.13 ± 0.04 mV/ms ($n = 10$). It increased by ≤40 and 25% in the presence of AKH I and AKH II, respectively (Fig. 5*D*). A half-maximal rise in slope was obtained with 29 pM AKH I and with 1.7 nM AKH II, respectively. Thus AKH I up-regulates spike activity and pacemaker slope more efficiently than AKH II. This is in contrast to the effect on hyperpolarization of the APs, which was potentiated by both peptides with very similar efficiency. The EC_{50} for this effect was 5.1 and 4.9 pM for AKH I and AKH II, respectively (Fig. 5*E*).

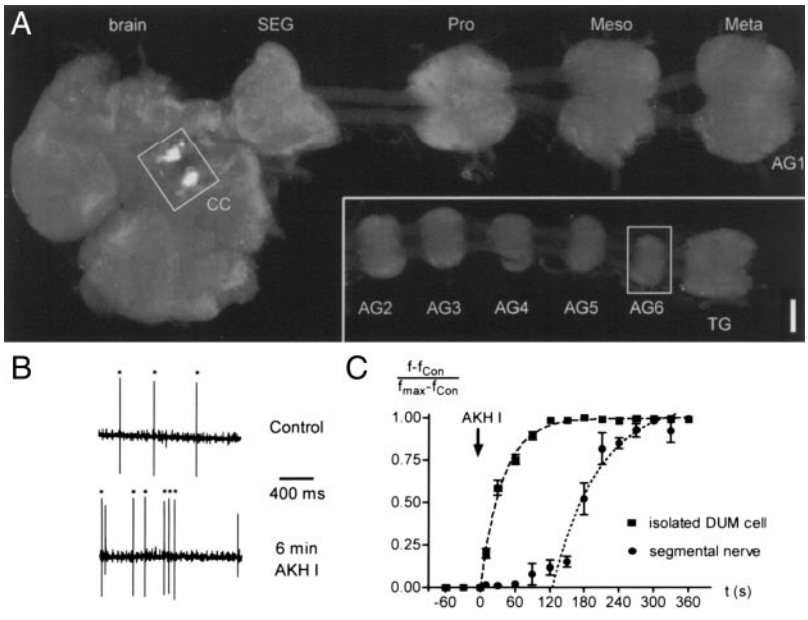

FIG. 4. AKH distribution and their crossing of the blood–brain barrier. *A*: anti-AKH I-like immunofluorescence in the embryonic *Periplaneta* nervous system (80% development) visualized with Cy3. Box between brain and subesophageal ganglion (SEG) indicates localization of the corpora cardiaca (CC). Posterior to the SEG are the prothoracic (Pro), the mesothoracic (Meso), the metathoracic (Meta), and the abdominal ganglia (AG) 1–6 followed by the terminal ganglion (TG). Note that only CC cells show immunoreactivity (*left box*), whereas there is no detectable fluorescence in the nervous system including the 6th abdominal ganglion (*right box*). Calibration bar: 100 μm. *B*: extracellular recordings from segmental nerve before and 6 min after application of 10 nM AKH I from outside of nervous system. Spikes marked with asterisks have a similar size and probably reflect the activity of 1 neuron. Note that, in the presence of AKH I, another neuron showing smaller spikes becomes active. *C*: diagram compares development of AKH I-induced acceleration of spiking in isolated DUM neurons ($n = 7$; cf. Fig. 5) and segmental nerve ($n = 7$). Data points are based on 10 registrations for 1 s in each preparation. In segmental nerve recordings, all large spikes were counted. Exponentials fitted to data according to *Eq. 3* are described by delay = 0 s and $\tau = 39$ s for DUM cells and delay = 126 s and $\tau = 80$ s for segmental nerve.

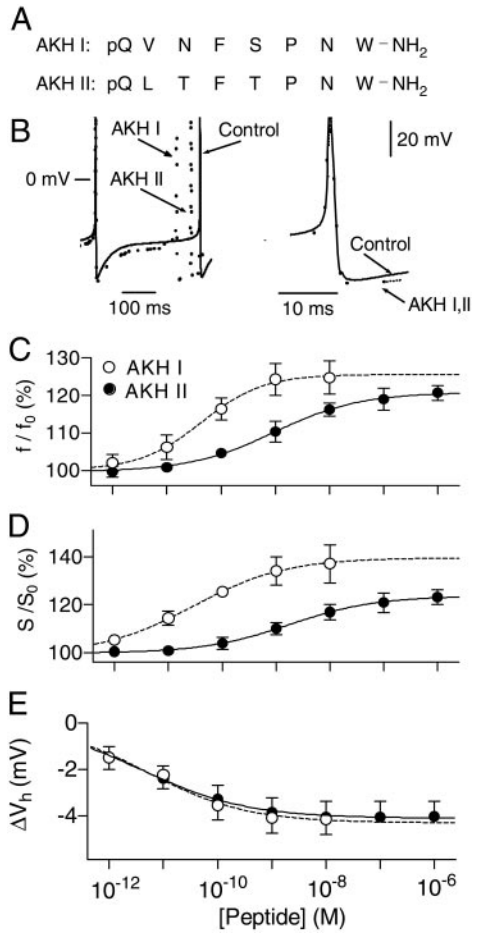

FIG. 5. Sequence of AKHs and their effects on electrical activity of DUM neurons. *A*: alignment of AKH peptides. Various names are used for these peptides, e.g., neurohormone D (Baumann and Penzlin 1984) or myotropin I (Witten et al. 1984) for AKH I and myotropin II for AKH II (Witten et al. 1984). *B*: action potentials recorded under current-clamp conditions (no current injected) before and 2 min after application of 1 nM AKH I or AKH II. While AKH I leads to a stronger acceleration of spiking (*left*), both peptides have the same effect on action potential hyperpolarization (*right*). *C*: spike frequencies, measured after peptide application, were normalized to frequencies registered in absence of peptides. Data represent $n = 10$ cells; in each cell, up to 3 concentrations were tested. Dose–response curves are described by an EC_{50} of 44 pM and 1.0 nM and a Hill coefficient (n_H) of 0.75 and 0.54 for AKH I and AKH II, respectively. *D*: relative change in pacemaker slope steepness, measured at −42 mV, the midpoint potential of interspike interval. Fit curves correspond to EC_{50} of 29 pM and 1.7 nM and n_H of 0.51 and 0.48 for AKH I and AKH II, respectively. *E*: increase in action potential hyperpolarization. Fit curves correspond to an EC_{50} of 5.1 and 4.9 pM and and n_H of 0.47 and 0.45 for AKH I and AKH II, respectively (*B–D*: $n = 7$ cells). Peptide effects (*C–E*) were statistically significant at concentrations >1 pM for AKH I and 10 pM for AKH II (paired *t*-test, $P < 0.05$).

Modulation by AKH peptides of ion currents in DUM neurons

The distinct effects of the two AKHs on the electrical activities of the DUM neurons suggest some differences in the modulations of the underlying ion currents. From previous studies, it was already known that AKH I affects a P/Q-type voltage-gated Ca^{2+} current (Wicher 2001b), a Na^+ current (Wicher 2001a), and a Ca^{2+} background current (Wicher et al. 2004). Hence, we compared how AKH I and AKH II affect these currents.

Voltage-gated Ca^{2+} channel currents

The somata of the abdominal DUM neurons express various voltage-gated Ca^{2+} channels (Grolleau and Lapied 1996; Wicher and Penzlin 1997). The Ca^{2+} current sensitive to the P/Q-type Ca^{2+} channel blockers ω-agatoxin IVA (ω-AgaTx) and ω-conotoxin MVIIC (ω-CmTx) is enhanced by AKH I (Wicher 2001b). The Ca^{2+} current induced by AKH I showed strong inactivation and was maximal at –20 mV (Fig. 6*A*). At this potential, only the P/Q-type current significantly contributes to the total Ca^{2+} current (Supplementary Fig. S3*C*; Wicher and Penzlin 1997). Application of 10 nM AKH II led to up-regulation of currents activating at voltages between –50 and 0 mV (Fig. 6*B*). With Sr^{2+} as a charge carrier, AKH II increased the current within the whole voltage range (Supplementary Fig. S3*A*), which is in line with the previously reported effect of AKH I (Wicher 2001b). The largest current increase was obtained at about –20 mV, and the current induced by AKH II inactivated rapidly (Fig. 6*A*; Supplementary Fig. S3*B*). To confirm that the effect of AKH II was restricted to the P/Q-type channel, we blocked this channel with 50 nM ω-AgaTx ($n = 4$) or 1 μM ω-CmTx ($n = 4$). Under these conditions, AKH II failed to enhance any Ca^{2+} current (Supplementary Fig. S3*C*) like previously shown for AKH I (Wicher 2001b). Thus both AKHs only affect the P/Q-type Ca^{2+} current.

To compare these AKH II effects quantitatively, we measured the current increase at –20 mV. AKH I and AKH II (both 10 nM) enhanced the Ca^{2+} current at –20 mV by 101 ± 33 ($n = 6$) and 119 ± 45% ($n = 5$), respectively. These figures were not significantly different (*t*-test). The midpoint potential of activation ($V_{0.5}$), which also reflects the contribution of the P/Q-type current to total Ca^{2+} current (Wicher and Penzlin 1997), was determined from the *I-V* relationships for peak currents taken before and 2 min after AKH application (*Eq. 1*). $V_{0.5}$ was shifted by AKH I and AKH II (10 nM) from –14 ± 2 to –19 ± 2 ($n = 6$) and –20 ± 2 mV ($n = 7$), respectively (difference statistically not significant). The slope remained unchanged in both cases. Thus AKH I and II were found to be equipotent in modulating this Ca^{2+} current. Also, the concentration dependence of peptide effects (Fig. 6*C*) was not significantly different (ANOVA, $P = 0.5$). The EC_{50} was 6.7 and 7.6 pM, and the saturating increase was 204 ± 7 and 212 ± 9% of control for AKH I and II, respectively.

Voltage-gated Na^+ channel currents

AKH I accelerates Na^+ channel inactivation kinetics, which in turn led to a reduction in current amplitude (Wicher 2001a). AKH II was found to act in the same manner: in the presence of 10 nM AKH II, the kinetics of activation of Na^+ current remained unchanged, whereas the amplitude of the current was reduced (Fig. 6*D*). AKH I and AKH II reduced the Na^+ current at –10 mV by 26 ± 8 ($n = 8$) and 23 ± 8% ($n = 5$), respectively (these figures were not significantly different, *t*-test). When comparing the *I-V* relation for peak currents under control conditions with that in the presence of AKHs, a voltage-dependence of peptide action becomes apparent (Fig. 6*E*). At lower depolarizations, at which the Na^+ current hardly inactivates, both AKHs have no effect on current amplitude. The current reduction starts at –20 mV and gains its full size at

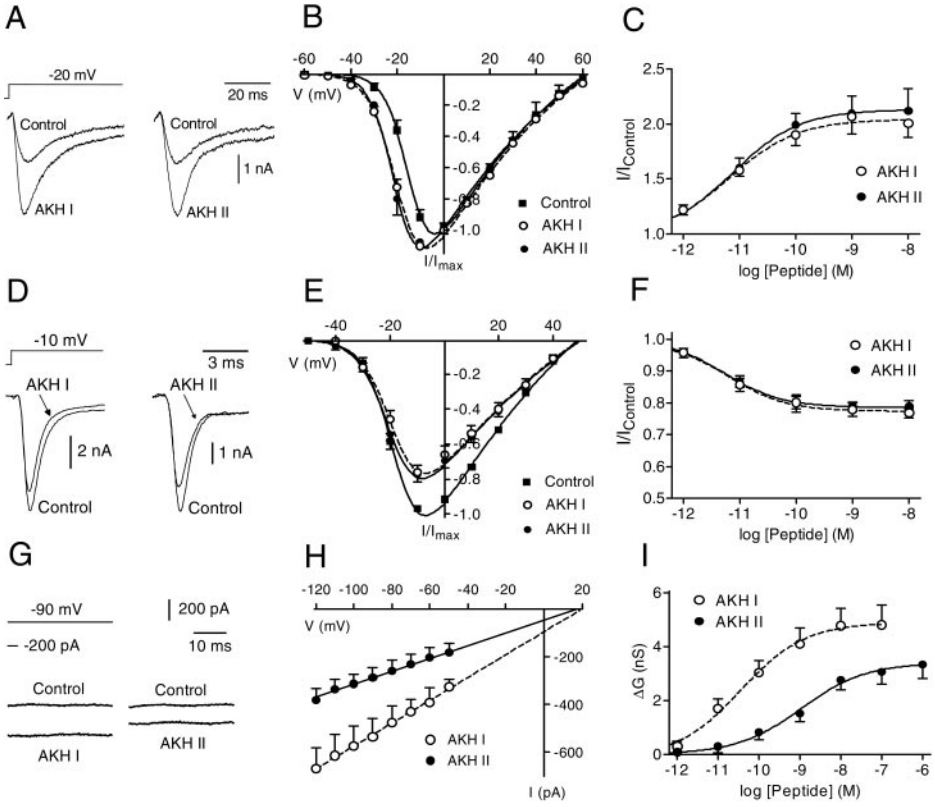

FIG. 6. AKH effect on voltage-gated Ca^{2+} and Na^{+} channels and on Ca^{2+} background currents in DUM neurons. *A*: Ca^{2+} current recordings obtained for the indicated pulse protocol before and after application of 10 nM AKH I and AKH II. *B*: *I-V* relationships for amplitudes of Ca^{2+} currents normalized to maxima obtained under control conditions ($n = 6$). Data were fit according to the GHK *Eq. 1* characterized by $V_{0.5}$ of –14, –19, and –20 mV and slope factor of 5.0, 5.8, and 5.0 mV for control, AKH I, and AKH II, respectively. *C*: concentration dependence of AKH-induced increase of Ca^{2+} current amplitudes at –20 mV ($n = 6$). Dose–response curves are described by an EC_{50} of 6.7 and 7.6 pM and n_H of 0.72 and 0.73 for AKH I and AKH II, respectively. *D*: Na^{+} current recordings obtained for indicated pulse protocol before and after application of 10 nM AKH I and AKH II. *E*: *I-V* relationships for Na^{+} currents normalized to maxima obtained under control conditions ($n = 7$). Data were fit according to the GHK *Eq. 1* characterized by $V_{0.5}$ of –17.2, –17.7, and –18.8 mV and by slope of 5.3, 5.6, and 5.6 mV for control, AKH I, and AKH II, respectively. *F*: concentration dependence of AKH-induced decrease of Na^{+} current amplitudes at –10 mV ($n = 6$). Dose–response curves are described by an IC_{50} of 6.2 and 5.3 pM and n_H of 0.85 and 0.84 for AKH I and AKH II, respectively. *G*: Ca^{2+} background current at –90 mV before and after application of 10 nM AKH I and AKH II. *H*: *I-V* relationship for currents produced by 10 nM AKH I and AKH II. Individual currents were recorded 40 ms after stepping to indicated voltages. *I* is difference between current recorded 2 min after peptide application and current recorded before ($n = 6$). Lines are results of linear regression analysis. *I*: concentration dependence of AKH-induced increase of Ca^{2+} background conductance ($n = 6$). Dose–response curves are described by an EC_{50} of 35 pM and 1.07 nM and n_H of 0.55 and 0.55 for AKH I and AKH II, respectively.

–5 mV (Fig. 6*E*). Both AKHs have no effect on the steady-state activation and inactivation (Supplementary Fig. S4). The concentration dependence of AKH actions on current amplitude were nearly identical for both peptides (Fig. 6*F*; ANOVA, $P = 0.55$). The IC_{50} was 6.2 and 5.3 pM, and the saturating reduction was 77 ± 1 and 78 ± 1% of controls for AKH I and II, respectively.

Ca^{2+} background current

As mentioned above, either peptide increased the steepness of the pacemaking depolarization in DUM neurons; however, in this respect, AKH II was less effective than AKH I (Fig. 5*D*). As previously found, AKH I potentiates a voltage-independent Ca^{2+}-selective background current (Wicher et al. 1994) that contributes to pacemaking (Wicher et al. 2004). Therefore we tested whether the peptides affect this current to a different extent. Both peptides produced an inward shift in current that was accompanied by an increase in input conductance. However, AKH II induced only one-half the size of the current observed with AKH I (Fig. 6*G*; 10 nM). The conductance produced by 10 nM AKH I was 4.77 ± 0.06 nS ($n = 6$), whereas AKH II generated only 2.67 ± 0.05 nS ($n = 6$; the difference between the *I-V* relations shown in Fig. 6*H* is statistically significant; ANOVA, $P < 0.0001$). Similarly, the dose–response curves for the increase in conductance by AKH I and AKH II were clearly different (Fig. 6*I*). The EC_{50} was 35 pM and 1.07 nM, and the saturating increase in conductance was 4.9 ± 0.4 and 3.4 ± 0.3 nS for AKH I and II, respectively.

Signal transduction systems involved in AKH actions

The modulation of P/Q-type Ca^{2+} channel by AKH I is caused by channel phosphorylation through protein kinase A (PKA) (Wicher 2001b). Also, the AKH I modulation of the Na^{+} channel was mediated by cAMP/PKA (Wicher 2001a).

The increase of Ca^{2+} background current by the AKH I was shown to require PLC activation (Wicher et al. 2004). To test whether AKH II operates through the same signal transduction pathway, we preincubated the neurons with the PLC inhibitor U73122 (3 μM). Under this condition, AKH II (10 nM) failed to affect this current ($n = 5$, data not shown).

Taken together, there was no difference in AKH effects on currents when the channels were modulated by phosphoryla-

tion by PKA, which is expected to originate from G_s protein activation. However, AKH II was less effective than AKH I when channels were modulated by the PLC cascade, i.e., when the AKHs are expected to induce G_q protein activation.

Effect of AKH peptides on locomotor activity

AKH release on starvation induces hyperactivity in *Drosophila* (Lee and Park 2004). To determine whether AKHs also affect locomotor activity of cockroaches, peptide injections into adult male *Periplaneta* were combined with running-wheel assays in constant darkness. To simulate the physiological AKH release into circulation, peptide and sham injections were placed into the thorax near the heart. About 1 h after an AKH I injection, there was a robust increase in locomotor activity that lasted for some hours (Fig. 7*A*). Control injections of dye into the thorax at the same location as the AKH I injections showed that it takes ≤1 h for the injected dye to appear in the ventral nerve cord. AKH II and sham injection hardly had an effect on locomotor activity. When comparing the mean locomotor activity up to 6 h after the respective injections, it became obvious that only AKH I significantly increased locomotor activity (Fig. 7*B*). For example, injection of AKH I during the resting phase enhanced a 60-fold increase in locomotor activity, whereas AKH II produced only a 9-fold increase. The effect of AKH II injection was not significantly different from that of sham injection (ANOVA, $P = 0.16$, $n = 8$). In general, the effect of AKHs was independent of the time of day, and it did not lead to phase shifts of the circadian locomotor activity rhythms (data not shown).

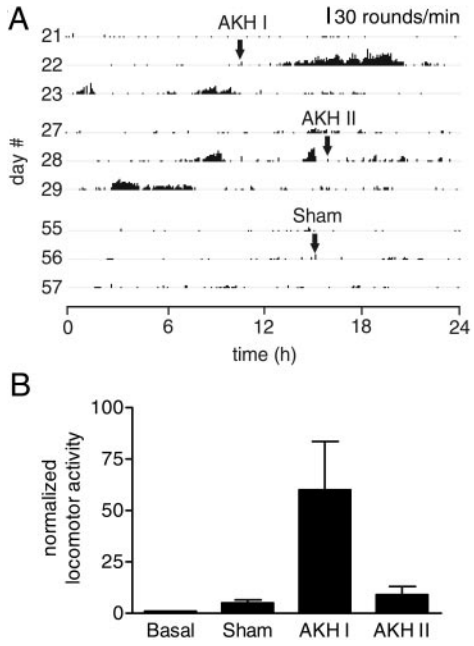

FIG. 7. AKH I stimulates the locomotor activity of *Periplaneta*. *A*: injection of AKHs (2 pmol) into *P. americana* near heart-enhanced locomotor activity independent of time of day. Sample registration of locomotor activity in a running wheel (given in rounds per minute, sampling interval 5 min) shows an increase in activity after injection of AKH I that lasts for 10 h. Injection of AKH II and sham injection had no visible effect. *B*: locomotor activity before (basal) and after sham and AKH injection (averaged for 6 h after injection). Data were normalized to basal activity. Sham ($n = 8$) and AKH II ($n = 5$) injection had no significant effect on activity, whereas AKH I ($n = 8$) injection significantly increased activity ($P = 0.03$).

DISCUSSION

There is a wealth of information on the role of AKHs in energy metabolism (Gäde and Auerswald 2003; Gäde et al. 1997; Van der Horst et al. 2001). However, there is emerging evidence that AKHs may also produce behavioral effects (Kodrik et al. 2000; Lee and Park 2004; Milde et al. 1995). Although it would be interesting to understand how AKHs orchestrate the various mechanisms underlying observable behavior, little is known about specific actions of AKHs within the nervous system. Some important advances in this respect derive from this study.

AKH acts from outside on nervous system

The AKH I antibody solely recognized endocrine cells of the CC, i.e., the cells already known to produce AKHs (Van der Horst et al. 2001). The observed lack of AKH-producing central neurons is in line with findings obtained for *Drosophila* (Kim and Rulifson 2004; Lee and Park 2004). Thus to act within the nervous system, AKHs have to penetrate the blood–brain barrier; this happened within a couple of minutes (Fig. 4*C*). It remains to be elucidated by which mechanism this is accomplished, i.e., by simple diffusion or active transport (Pan and Kastin 2004).

Neuronal AKH receptors

We showed for the first time that AKHRs are expressed within the insect CNS. The widespread occurrence of the receptor may seem intriguing and asks for further study, yet for the present purpose, it is of prime importance that AKHR is expressed in the DUM neurons.

Because DUM neurons in abdominal ganglia are spontaneously active and release octopamine, any changes in their spiking might have pronounced effects in two respects: First, the animal's general activity level may be affected because DUM neurons are part of the general, octopaminergic, arousal system (Roeder 2005). General arousal induced by AKH through an increase in the level of octopamine probably involves the stimulation of a large number of cells. In line with this, it was previously observed that AKH I also stimulates DUM neurons in the terminal abdominal ganglion (Wicher et al. 1994).

Second, through their specific projections, the abdominal DUM neurons act in a supportive manner on respiration and circulation to adapt the animal to increased motor activity. More complex roles have been established for thoracic DUM neurons: in the locust, the subsets of DUM neurons supplying the wing muscles are inhibited during flight while other DUM cells are active (Duch et al. 1999; Pflüger 1999). Octopamine has an additional direct effect on the fuel selection of wing muscles where it leads, during prolonged flight, to a switch from carbohydrate to lipid as the main fuel (Mentel et al. 2003).

Effects of adipokinetic hormones: from receptor activation to modulation of neuronal activity

The two AKHs in cockroach differently affect the spiking of DUM neurons. While they are equipotent in enhancing the hyperpolarization, the frequency of spiking is increased more

strongly by AKH I compared with AKH II. A straightforward explanation of the peptide effects on spiking of DUM neurons is offered by their modulatory effects on ion currents observed both in HEK293 cells expressing pAKHR and in abdominal DUM neurons.

The shape of the action potential is an important factor determining the release of messengers by a neuron (e.g., Borst and Sakmann 1999). Both AKHs increased the hyperpolarization with the same concentration dependence (Fig. 5E). The AKH I-effect on hyperpolarization results from up-regulation of a Ca^{2+}-dependent K^+ current (Wicher 2001b; Wicher et al. 1994) conducted by a Slo channel (Derst et al. 2003). The increase in this K^+ current reflects the AKH I–induced potentiation of the P/Q-type Ca^{2+} current, resulting from AKH receptor coupling to G_s because it is transduced by activation of adenylate cyclase/PKA (Wicher 2001b). In the heterologous expression system, both AKHs induced AKH receptor coupling to G_s with equal potency. One would expect that they equally modulate voltage-gated Ca^{2+} channels in DUM neurons. This, indeed, was seen to be the case (Fig. 6, *A–C*).

AKH peptides also modify voltage-gated Na^+ channels in DUM neurons. Again this is caused by channel phosphorylation by PKA (Wicher 2001a) and, hence, also reflects AKH receptor coupling to G_s. In line with this, the modulation of the Na^+ current by AKH II did not differ from that by AKH I (Fig. 6, *D–F*). The peptidergic modification of Na^+ current that causes a reduced Na^+ influx leads to an attenuation of Na^+-dependent K^+ current (Wicher et al. 2006).

In a previous study, we quantified the AKH I–induced changes in ion currents in terms of Hodgkin-Huxley models and simulated the resulting activity of DUM neurons (Wicher et al. 2006). Up-regulation of P/Q-type Ca^{2+} and Ca^{2+}-dependent K^+ current enhanced the hyperpolarization but had a weak effect on spiking. Down-regulation of Na^+ and Na^+-dependent K^+ current decreased hyperpolarization and slightly accelerated spiking. Superposition of these modulations produced an increased hyperpolarization while the spike frequency remained unchanged. Only when the up-regulation of the pacemaking Ca^{2+} background current was included in the simulation did the model reproduce the experimentally observed AKH I–induced changes (Wicher et al. 2006). Thus the similar effects of both AKHs on action potential hyperpolarization arise from the equal potency of both peptides to induce G_s coupling of the AKH receptor.

AKH I and, less potently AKH II, accelerated spiking of DUM neurons (Fig. 5*C*). This was reflected by the increased steepness of the pacemaker slope, which was weaker with AKH II than with AKH I. The AKH I effect on pacemaking arises from the potentiation of a Ca^{2+} background current (Heine and Wicher 1998). The involved signal transduction mechanism includes activation of PLC (Wicher et al. 2004) and thus most probably reflects coupling of the AKH receptor to G_q. AKH I was clearly more efficient in up-regulating the Ca^{2+} background current than AKH II (Fig. 6, *G–I*).

The concentration dependencies of AKH effects on spiking were found to be in good accordance to the corresponding effects on ion currents. That is, the virtually identical dose–response of both AKHs on hyperpolarization corresponds to the dose–response for P/Q-type Ca^{2+} currents and Na^+ current modulation, whereas the different dose–response for the acceleration of spiking and increase in pacemaker depolarization was mirrored by the different dose–response for Ca^{2+} background current increase.

We have thus shown that both the similarity and the difference of the neuronal effects of AKHs can be explained by a different capability to activate the receptor: AKH binding leads to receptor coupling to both G_s and G_q. While both AKHs have similar potency to stimulate activation of G_s, AKH II is less potent than AKH I in stimulating G_q activation (Fig. 1). There are various examples for promiscuous receptor coupling to G protein α subunits (Kiselyov et al. 2003), among them a *Drosophila* octopamine/tyramine receptor (Evans et al. 1995; Robb et al. 1994) and the mammalian GnRH receptor that is structurally related to the AKH receptor (Liu et al. 2002). gonadotropin releasing hormone (GnRH) I and II binding to the human GnRH receptor may differentially stabilize different receptor active conformations that leads to differential signaling (Lu et al. 2005).

G_q coupling of the *Drosophila* AKH receptor, dAKHR, has previously been shown using *Xenopus* oocytes (Park et al. 2002). The activity of AKHs in fat body cells involves the interaction of activated AKHRs with both, G_s and G_q: While G_s coupling is a precondition for lipid mobilization, carbohydrate mobilization requires coupling to G_q (Gäde and Auerswald 2003).

There is a remarkable difference in the EC_{50} values for the G_s- and G_q-mediated effects of AKH peptides. While the EC_{50} for the G_s-mediated increase in hyperpolarization by AKH I was 5 pM, it was 44 pM for the G_q-mediated acceleration of spiking (Fig. 5). A similar difference was observed for the effects of GnRH in hypothalamic GnRH neurons (Krsmanovic et al. 2003), where the increase in cAMP level caused by G_s activation was maximal at 1 nM GnRH and the rise in inositoltrisphosphate level caused by G_q activation required $\geq$10 nM GnRH and saturated at 1 μM GnRH.

AKH and locomotor activity

The regulation of energy balance including food acquisition is essential for survival of an animal. AKHs are known to stimulate energy mobilization on prolonged activity (Gäde et al. 1997). AKH producing and releasing CC cells in *Drosophila* sense the blood glucose level through ATP-sensitive K^+ channels, i.e., by the same mechanism used by mammalian glucose-sensing cells (Kim and Rulifson 2004). An energy deficiency on starvation produced enhanced locomotor activity in *Drosphila* independently of the basal circadian activity (Lee and Park 2004). Such behavior seems to be a reasonable strategy to support the search for food sources.

While in *Drosphila* there is only one AKH, up to three AKH peptides with overlapping functions with respect to their metabolic action, i.e., lipid or carbohydrate mobilization, may occur in one insect species (Gäde and Auerswald 2003). *Locusta* AKH I, for example, is much more potent in lipid mobilization than AKH II and III (Goldsworthy et al. 1997). In *Periplaneta,* we found a clear difference between the behavioral effect of AKH I and II. While AKH I strongly stimulated locomotor activity, there was hardly any effect of AKH II. For comparison, both peptides equally mobilize carbohydrates (Scarborough et al. 1984). We thus propose that the two AKHs play different physiological roles. Only AKH I may function as

a stress message and induces behavior on metabolic demand to support fight or flight.

That only AKH I effectively stimulates locomotor activity in the cockroach strikingly corresponds with its stronger potentiation of the pacemaking Ca^{2+} background current and its stronger effect on DUM cell spiking. Presently we do not know the chain of events from (in our case: artificial) a rise in blood AKH to the increased activity of locomotor pattern generator(s) (Büschges 2005). One possibility may be a direct AKH effect on such sets of neurons, and if so, one may assume that they exhibit a similar Ca^{2+} background current that is affected in a similar way by AKH I.

An alternative—which we consider more likely—is that an enhanced release of octopamine from DUM neurons feeds forward on "decision making" neurons endowed with appropriate octopamine receptors (Evans and Maqueira 2005). This possibility would be strengthened if one could show that most, if not all, DUM neurons are activated by AKH. The rise of the octopamine level in the hemolymph might take some time and thus account, in addition to the time required for AKH to approach the nervous system, for the long latency of the increase in motor activity. Also one has to take into account that octopamine can induce AKH release, e.g., during prolonged flight (Roeder 2005). This opens the possibility of a positive feedback: more AKH → more octopamine → more AKH → more octopamine and so on. In addition, one has to take into account that abdominal DUM neurons can be excited by octopamine, which would further drive such a positive feedback, yet not "indefinitely," because that octopamine effect changes to an inhibitory one when the octopamine becomes very high (Achenbach et al. 1997).

Clearly, considerable further work is required to dissect and clarify the interdependence of such neuroendocrine mechanisms to understand the "simple" fact that AKH can lead to increased locomotion.

ACKNOWLEDGMENTS

The authors thank S. Arendt, S. Kaltofen, G. Radtke, A. Roβner, and A. Schmidt for technical assistance, Dr. M. Biel for the gift of hHCN2 DNA, and Dr. C. Walther for critical discussion of the manuscript.

GRANTS

This work was supported by the Deutsche Forschungsgemeinschaft (Wi 1422/2–4.5).

REFERENCES

Accili EA, Proenza C, Baruscotti M, and DiFrancesco D. From funny current to HCN channels: 20 years of excitation. *News Physiol Sci* 17: 32–37, 2002.

Achenbach H, Walther C, and Wicher D. Octopamine modulates ionic currents and spiking in dorsal unpaired median (DUM) neurons. *Neuroreport* 8: 3737–3741, 1997.

Bacon JP and Altman JS. A silver intensification method for cobalt-filled neurones in wholemount preparations. *Brain Res* 138: 359–363, 1977.

Baumann E and Penzlin H. Sequence analysis of neurohormone D, a neuropeptide of an insect, Periplaneta americana. *Biomed Biochim Acta* 43: K13–K16, 1984.

Borst JG and Sakmann B. Effect of changes in action potential shape on calcium currents and transmitter release in a calyx-type synapse of the rat auditory brainstem. *Philos Trans R Soc Lond B Biol Sci* 354: 347–355, 1999.

Bräunig P and Pflüger H-J. The unpaired median neurons of insects. *Adv Insect Physiol* 28: 185–266, 2001.

Büschges A. Sensory control and organization of neural networks mediating coordination of multisegmental organs for locomotion. *J Neurophysiol* 93: 1127–1135, 2005.

Daaka Y, Luttrell LM, and Lefkowitz RJ. Switching of the coupling of the beta2-adrenergic receptor to different G proteins by protein kinase A. *Nature* 390: 88–91, 1997.

Dacks AM, Christensen TA, Agricola HJ, Wollweber L, and Hildebrand JG. Octopamine-immunoreactive neurons in the brain and subesophageal ganglion of the hawkmoth *Manduca sexta. J Comp Neurol* 488: 255–268, 2005.

Derst C, Messutat S, Walther C, Eckert M, Heinemann SH, and Wicher D. The large conductance Ca^{2+}-activated potassium channel (pSlo) of the cockroach *Periplaneta americana*: structure, localisation in neurones and electrophysiology. *Eur J Neurosci* 17: 1197–1212, 2003.

Duch C, Mentel T, and Pflüger HJ. Distribution and activation of different types of octopaminergic DUM neurons in the locust. *J Comp Neurol* 403: 119–134, 1999.

Eckert M, Gabriel J, Birkenbeil H, Greiner G, Rapus J, and Gäde G. A comparative immunocytochemical study using an antiserum against a synthetic analogue of the corpora cardiaca peptide Pea-CAH-I (MI, neurohormone D) of *Periplaneta americana. Cell Tissue Res* 284: 401–413, 1996.

Eckert M, Rapus J, Nürnberger A, and Penzlin H. A new specific antibody reveals octopamine-like immunoreactivity in cockroach ventral nerve cord. *J Comp Neurol* 322: 1–15, 1992.

Evans PD and Maqueira B. Insect octopamine receptors: a new classification scheme based on studies of cloned *Drosophila* G-protein coupled receptors. *Invert Neurosci* 5: 111–118, 2005.

Evans PD, Robb S, Cheek TR, Reale V, Hannan FL, Swales LS, Hall LM, and Midgley JM. Agonist-specific coupling of G-protein-coupled receptors to second-messenger systems. *Prog Brain Res* 106: 259–268, 1995.

Ferber M and Pflüger HJ. An identified dorsal unpaired median neurone and bilaterally projecting neurones exhibiting bovine pancreatic polypeptide-like/FMRFamide-like immunoreactivity in abdominal ganglia of the migratory locust. *Cell Tissue Res* 267: 85–98, 1992.

Gäde G, and Auerswald L. Mode of action of neuropeptides from the adipokinetic hormone family. *Gen Comp Endocrinol* 132: 10–20, 2003.

Gäde G, Hoffmann KH, and Spring JH. Hormonal regulation in insects: facts, gaps, and future directions. *Physiol Rev* 77: 963–1032, 1997.

Goldsworthy GJ, Lee MJ, Luswata R, Drake AF, and Hyde D. Structures, assays and receptors for locust adipokinetic hormones. *Comp Biochem Physiol B Biochem Mol Biol* 117: 483–496, 1997.

Grolleau F and Lapied B. Two distinct low-voltage-activated Ca^{2+} currents contribute to the pacemaker mechanism in cockroach dorsal unpaired median neurons. *J Neurophysiol* 76: 963–976, 1996.

Grolleau F and Lapied B. Dorsal unpaired median neurones in the insect central nervous system: towards a better understanding of the ionic mechanisms underlying spontaneous electrical activity. *J Exp Biol* 203: 1633–1648, 2000.

Heine M and Wicher D. Ca^{2+} resting current and Ca^{2+}-induced Ca^{2+} release in insect neurosecretory neurons. *Neuroreport* 9: 3309–3314, 1998.

Kim SK and Rulifson EJ. Conserved mechanisms of glucose sensing and regulation by *Drosophila* corpora cardiaca cells. *Nature* 431: 316–320, 2004.

Kiselyov K, Shin DM, and Muallem S. Signalling specificity in GPCR-dependent Ca^{2+} signalling. *Cell Signal* 15: 243–253, 2003.

Kodrik D, Socha R, Simek P, Zemek R, and Goldsworthy GJ. A new member of the AKH/RPCH family that stimulates locomotory activity in the firebug, *Pyrrhocoris apterus* (Heteroptera). *Insect Biochem Mol Biol* 30: 489–498, 2000.

Krsmanovic LZ, Mores N, Navarro CE, Arora KK, and Catt KJ. An agonist-induced switch in G protein coupling of the gonadotropin-releasing hormone receptor regulates pulsatile neuropeptide secretion. *Proc Natl Acad Sci USA* 100: 2969–2974, 2003.

Lapied B, Malecot CO, and Pelhate M. Ionic species involved in the electrical activity of single adult aminergic neurons isolated from the sixth abdominal ganglion of the cockroach *Periplaneta americana. J Exp Biol* 144: 535–550, 1989.

Lee G and Park JH. Hemolymph sugar homeostasis and starvation-induced hyperactivity affected by genetic manipulations of the adipokinetic hormone-encoding gene in *Drosophila melanogaster. Genetics* 167: 311–323, 2004.

Liu F, Usui I, Evans LG, Austin DA, Mellon PL, Olefsky JM, and Webster NJ. Involvement of both $G_{q/11}$ and G_s proteins in gonadotropin-releasing hormone receptor-mediated signaling in L beta T2 cells. *J Biol Chem* 277: 32099–32108, 2002.

Lu ZL, Gallagher R, Sellar R, Coetsee M, and Millar RP. Mutations remote from the human gonadotropin-releasing hormone (GnRH) receptor-binding

sites specifically increase binding affinity for GnRH II but not GnRH I: evidence for ligand-selective, receptor-active conformations. *J Biol Chem* 280: 29796–29803, 2005.

Ludwig A, Zong X, Stieber J, Hullin R, Hofmann F, and Biel M. Two pacemaker channels from human heart with profoundly different activation kinetics. *EMBO J* 18: 2323–2329, 1999.

Mentel T, Duch C, Stypa H, Wegener G, Müller U, and Pflüger HJ. Central modulatory neurons control fuel selection in flight muscle of migratory locust. *J Neurosci* 23: 1109–1113, 2003.

Milde JJ, Ziegler R, and Wallstein M. Adipokinetic hormone stimulates neurones in the insect central nervous system. *J Exp Biol* 198: 1307–1311, 1995.

Nässel DR. Neuropeptides, amines and amino acids in an elementary insect ganglion: functional and chemical anatomy of the unfused abdominal ganglion. *Prog Neurobiol* 48: 325–420, 1996.

Pan W and Kastin AJ. Polypeptide delivery across the blood-brain barrier. *Curr Drug Targets CNS Neurol Disord* 3: 131–136, 2004.

Park Y, Kim YJ, and Adams ME. Identification of G protein-coupled receptors for *Drosophila* PRXamide peptides, CCAP, corazonin, and AKH supports a theory of ligand-receptor coevolution. *Proc Natl Acad Sci USA* 99: 11423–11428, 2002.

Pflüger HJ. Neuromodulation during motor development and behavior. *Curr Opin Neurobiol* 9: 683–689, 1999.

Robb S, Cheek TR, Hannan FL, Hall LM, Midgley JM, and Evans PD. Agonist-specific coupling of a cloned *Drosophila* octopamine/tyramine receptor to multiple second messenger systems. *EMBO J* 13: 1325–1330, 1994.

Roeder T. Tyramine and octopamine: ruling behavior and metabolism. *Annu Rev Entomol* 50: 447–477, 2005.

Sakai M and Yamaguchi T. Differential staining of insect neurons with nickel and cobalt. *J Insect Physiol* 29: 393–397, 1983.

Saraswati S, Fox LE, Soll DR, and Wu CF. Tyramine and octopamine have opposite effects on the locomotion of *Drosophila* larvae. *J Neurobiol* 58: 425–441, 2004.

Scarborough RM, Jamieson GC, Kalish F, Kramer SJ, McEnroe GA, Miller CA, and Schooley DA. Isolation and primary structure of two peptides with cardioacceleratory and hyperglycemic activity from the corpora cardiaca of *Periplaneta americana. Proc Natl Acad Sci USA* 81: 5575–5579, 1984.

Schooneveld H, Tesser GI, Veenstra JA, and Romberg-Privee HM. Adipokinetic hormone and AKH-like peptide demonstrated in the corpora cardiaca and nervous system of *Locusta migratoria* by immunocytochemistry. *Cell Tissue Res* 230: 67–76, 1983.

Selyanko AA, Hadley JK, Wood IC, Abogadie FC, Jentsch TJ, and Brown DA. Inhibition of KCNQ1-4 potassium channels expressed in mammalian cells via M1 muscarinic acetylcholine receptors. *J Physiol* 522: 349–355, 2000.

Sgourakis NG, Bagos PG, Papasaikas PK, and Hamodrakas SJ. A method for the prediction of GPCRs coupling specificity to G-proteins using refined profile hidden Markov models. *BMC Bioinform* 6: 104, 2005.

Staubli F, Jorgensen TJ, Cazzamali G, Williamson M, Lenz C, Sondergaard L, Roepstorff P, and Grimmelikhuijzen CJ. Molecular identification of the insect adipokinetic hormone receptors. *Proc Natl Acad Sci USA* 99: 3446–3451, 2002.

Stengl M and Homberg U. Pigment-dispersing hormone-immunoreactive neurons in the cockroach *Leucophaea maderae* share properties with circadian pacemaker neurons. *J Comp Physiol [A]* 175: 203–213, 1994.

Stevenson PA, Dyakonova V, Rillich J, and Schildberger K. Octopamine and experience-dependent modulation of aggression in crickets. *J Neurosci* 25: 1431–1441, 2005.

Van der Horst DJ, Van Marrewijk WJ, and Diederen JH. Adipokinetic hormones of insect: release, signal transduction, and responses. *Int Rev Cytol* 211: 179–240, 2001.

Wicher D. Peptidergic modulation of an insect Na^+ current: role of protein kinase A and protein kinase C. *J Neurophysiol* 85: 374–383, 2001a.

Wicher D. Peptidergic modulation of insect voltage-gated Ca^{2+} currents: role of resting Ca^{2+} current and protein kinases A and C. *J Neurophysiol* 86: 2353–2362, 2001b.

Wicher D, Berlau J, Walther C, and Borst A. Peptidergic counter-regulation of Ca^{2+}- and Na^+-dependent K^+ currents modulates the shape of action potentials in neurosecretory insect neurons. *J Neurophysiol* 95: 311–322, 2006.

Wicher D, Messutat S, Lavialle C, and Lapied B. A new regulation of non-capacitative calcium entry in insect pacemaker neurosecretory neurons. Involvement of arachidonic acid, no-guanylyl cyclase/cGMP, and cAMP. *J Biol Chem* 279: 50410–50419, 2004.

Wicher D and Penzlin H. Ca^{2+} currents in central insect neurons: electrophysiological and pharmacological properties. *J Neurophysiol* 77: 186–199, 1997.

Wicher D, Walther C, and Penzlin H. Neurohormone D induces ionic current changes in cockroach central neurones. *J Comp Physiol [A]* 174: 507–515, 1994.

Wicher D, Walther C, and Wicher C. Non-synaptic ion channels in insects - basic properties of currents and their modulation in neurons and skeletal muscles. *Prog Neurobiol* 64: 431–525, 2001.

Witten JL, Schaffer MH, O'Shea M, Cook JC, Hemling ME, and Rinehart KL Jr. Structures of two cockroach neuropeptides assigned by fast atom bombardment mass spectrometry. *Biochem Biophys Res Commun* 124: 350–358, 1984.

Yabuki Y, Muramatsu T, Hirokawa T, Mukai H, and Suwa M. GRIFFIN: a system for predicting GPCR-G-protein coupling selectivity using a support vector machine and a hidden Markov model. *Nucleic Acids Res* 33: W148–W153, 2005.